Spin Polarization of Rb and Cs np $^{2}P_{3/2}$ (n=5, 6) Atoms by Circularly Polarized Photoexcitation of a Transient Diatomic Molecule

A. E. Mironov, J. D. Hewitt, and J. G. Eden

Spin Polarization of Rb and Cs $np\,{}^2\mathrm{P}_{\frac{3}{2}}$ (n=5,6) Atoms by Circularly-Polarized Photoexcitation of a Transient Diatomic Molecule

A. E. Mironov,[1, *] J. D. Hewitt,[2] and J. G. Eden[1]

[1]Laboratory for Optical Physics and Engineering,
Department of Electrical and Computer Engineering, University of Illinois, Urbana, IL 61801, USA
[2]Department of Engineering and Physics, Abilene Christian University, Abilene, TX 79699, USA
(Dated: September 2016)

We report the selective population of Rb or Cs $np\,{}^2\mathrm{P}_{\frac{3}{2}}$ ($n = 5, 6; F = 4, 5$) hyperfine states by the photodissociation of a transient, alkali-rare gas diatomic molecule. Circularly-polarized (σ^-), amplified spontaneous emission (ASE) on the D_2 line of Rb or Cs (780.0 and 852.1 nm, respectively) is generated when Rb-Xe or Cs-Xe ground state collision pairs are photoexcited by a σ^+-polarized optical field having a wavelength within the D_2 blue satellite continuum, associated with the $B\,{}^2\Sigma_{\frac{1}{2}}^+ \longleftarrow X\,{}^2\Sigma_{\frac{1}{2}}^+$ (free$\longleftarrow$free) transition of the diatomic molecule. The degree of spin polarization of Cs ($6p\,{}^2\mathrm{P}_{\frac{3}{2}}$), specifically, is found to be dependent on the interatomic distance (R) at which the excited complex is born, a result attributed to the structure of the $B\,{}^2\Sigma_{\frac{1}{2}}^+$ state. For Cs-Xe atomic pairs, tuning the wavelength of the optical field from 843 nm to 848 nm varies the degree of circular polarization of the ASE from 63% to almost unity because of the perturbation, in the $5 \leq R \leq 6$ Å interval, of the ${}^2\Sigma_{\frac{1}{2}}^+$ potential by a $d\sigma$ molecular orbital associated with a higher ${}^2\Lambda$ electronic state. Monitoring only the Cs $6p\,{}^2\mathrm{P}_{\frac{3}{2}}$ spin polarization reveals a previously unobserved interaction of CsXe ($B\,{}^2\Sigma_{\frac{1}{2}}^+$) with the lowest vibrational levels of a ${}^2\Lambda$ state derived from Cs ($5d$)+Xe. By inserting a molecular intermediate into the alkali atom excitation mechanism, these experiments realize electronic spin polarization through populating no more than two $np\,{}^2\mathrm{P}_{\frac{3}{2}}$ hyperfine states, and demonstrate a sensitive spectroscopic probe of R-dependent state-state interactions and their impact on interatomic potentials.

PACS numbers:

Spin polarization of atoms with circularly-polarized optical fields [1] has proven to be a powerful tool for magnetometry [2, 3], optical field-matter interactions [4], astrophysics [5], and generating hyperpolarized nuclei by spin exchange [6, 7]. Several decades following the initial experiments of Hanle [8] in which the depolarization of Hg 253.7 nm resonance radiation was observed, spin polarization of Na in a rare gas background was studied [9] and the production of polarized ^{3}He nuclei from optically-pumped Rb atoms was reported [6]. Since that time, spin polarization of the alkali atoms by photoexciting the D_1 or D_2 atomic resonance transitions with circularly-polarized radiation has become the basis for biomedical imaging with hyperpolarized ^{129}Xe or ^{3}He nuclei realized by spin-exchange with Rb or Cs [10–12]. Typically, spin polarization in the alkalis has been established in the $ns\,{}^2\mathrm{S}_{\frac{1}{2}}$ ground state ($n = 4 - 6$ for K, Rb, and Cs, respectively) by depopulation optical pumping [1, 10] in which the population of a specific ground state hyperfine level is selectively depleted by circularly-polarized optical excitation of the D_1 atomic transition ($np\,{}^2\mathrm{P}_{\frac{1}{2}} \longleftarrow ns\,{}^2\mathrm{S}_{\frac{1}{2}}$). Aside from pumping the alkali excited states directly from ground, virtually all previous experiments have required the imposition of an external magnetic field, and the degree of spin polarization could not be determined from atomic fluorescence.

We report here the electronic spin polarization of Rb and Cs $np\,{}^2\mathrm{P}_{\frac{3}{2}}$ atoms by the photoexcitation and subsequent dissociation of a transient diatomic molecule. Amplified spontaneous emission (ASE) is observed on the $np\,{}^2\mathrm{P}_{\frac{3}{2}} \longrightarrow ns\,{}^2\mathrm{S}_{\frac{1}{2}}$ (D_2) line of the alkali atom (780.0 nm and 852.1 nm for Rb and Cs, respectively) when thermal Rb-Xe or Cs-Xe ground state pairs are photoassociated with circularly-polarized (σ^+) laser radiation having a wavelength lying within the D_2 blue satellite continuum ($\sim 840.3 - 850.0$ nm for Cs-Xe). Also circularly-polarized, the D_2 line ASE demonstrates that the subsequent dissociation of the $B\,{}^2\Sigma_{\frac{1}{2}}^+$ alkali-rare gas diatomic complex populates preferentially the $F = 4, 5$ ($\mathrm{m_J} = \frac{1}{2}, \frac{3}{2}$; I = 7/2) hyperfine sublevels of the Cs $6p\,{}^2\mathrm{P}_{\frac{3}{2}}$ state, for example. Thus, electronic spin polarization is produced in the alkali $np\,{}^2\mathrm{P}_{\frac{3}{2}}$ excited state (as opposed to ground) and the degree of polarization is monitored directly through the ASE generated. Virtually all of the $np\,{}^2\mathrm{P}_{\frac{3}{2}}$ population resides in two hyperfine states, owing primarily to the choice of a ${}^2\Sigma^+$ potential as the terminal molecular state for the photoexcitation of alkali-rare gas atomic pairs. Because the spin vector $\vec{S}$ for the $B\,{}^2\Sigma_{\frac{1}{2}}^+$ potential is decoupled from the internuclear axis, the optical pumping approach reported here is not only capable of realizing circular polarization of the alkali D_2 line ASE approaching 100% with a broadband optical field, but slight deviations in the local molecu-
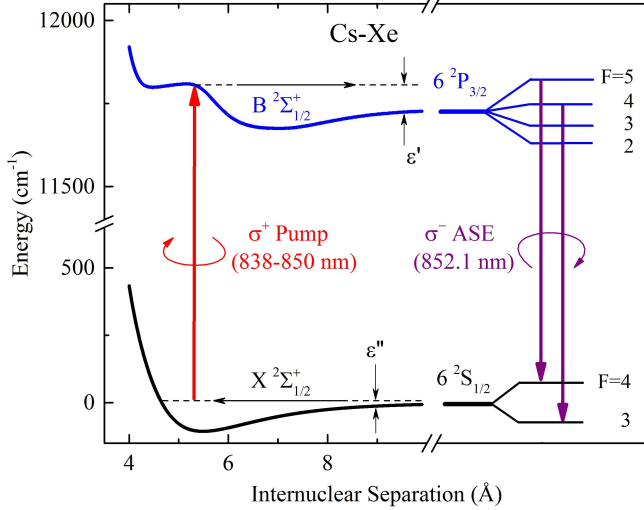
FIG. 1: Partial energy level diagram for the Cs-Xe diatomic complex, illustrating the photoassociation of ground state Cs-Xe collision pairs with a LHCP (σ^+) optical field, thereby forming a transient molecule in the $B\,^2\Sigma^+_{\frac{1}{2}}$ state. Subsequent dissociation of the excited complex yields a spin-polarized, alkali atomic fragment. For clarity, the bound $A\,^2\Pi_{\frac{1}{2}}$ and $A\,^2\Pi_{\frac{3}{2}}$ molecular states are not shown, but an expanded view of the hyperfine structure of the Cs $6\,^2S_{\frac{1}{2}}$ and $6\,^2P_{\frac{3}{2}}$ states is given at right (not to scale). The X and B interatomic potentials shown are those calculated on the basis of absorption spectra (Ref. [14])

lar orbital composition of the B state from $^2\Sigma^+$ character are readily detectable. In the present experiments, photoassociating Cs-Xe pairs, for example, through the $B\,^2\Sigma^+_{\frac{1}{2}} \longleftarrow X\,^2\Sigma^+_{\frac{1}{2}}$ continuum yields Cs $6\,^2P_{\frac{3}{2}}$ spin polarizations varying continuously between 63% and $> 95\%$ as the pump laser is tuned from ~ 843 nm to 848 nm. Doing so scans the Franck-Condon region in which the atomic collision pairs are photoexcited. The partial depolarization of the D_2 line ASE in the $5 \leq R \leq 6$ Å interval is attributed to the localized influence of a $d\sigma$ molecular orbital (originating from a higher energy molecular state) on the $B\,^2\Sigma^+_{\frac{1}{2}}$ potential. Predicted by Pascale and Vandeplanque [13] in 1974, the state-state perturbation reported here has not been observed previously.

Figure 1 is a partial energy level diagram of the CsXe diatomic molecule, illustrating two electronic states correlated with Cs($6s, 6p$)+Xe($5p^6\,^1S_0$) in the separated atom limit [13, 14]. As discussed below, ASE is observed on the D_2 transition of Cs and Rb when photoexcitation of alkali-rare gas collision pairs is driven by a σ^+ optical field. Thermal Cs ($6s\,^2S_{\frac{1}{2}}$) and Xe ($5p^6\,^1S_0$) atoms approach each other along the $X\,^2\Sigma^+_{\frac{1}{2}}$ ground state potential, and photoassociating these collision pairs with a left-hand, circularly-polarized optical field (LHCP, σ^+) having a wavelength in the alkali D_2
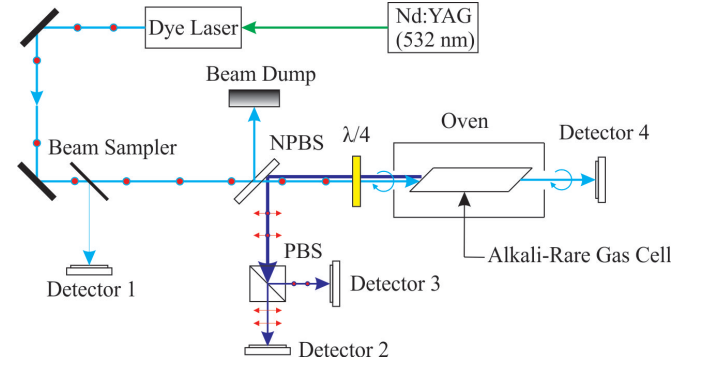

FIG. 2: Schematic diagram of the experimental arrangement with which the energies of the horizontal and vertical components of the backward wave ASE are measured.

blue satellite populates the dissociative $B\,^2\Sigma^+_{\frac{1}{2}}$ state of the diatomic molecule. Such free$\longleftarrow$free transitions of the alkali-rare gas complex occur in a Franck-Condon region determined by the wavelength (λ) of the pump radiation and the $B - X$ difference potential [15–17]. From a semiclassical perspective, the photoassociation of thermal atomic pairs occurs predominantly in regions of interatomic separation (R) in which $\epsilon' = \epsilon''$, where ϵ' and ϵ'' are the translational energies of the outgoing Cs($6p$)-Xe and incoming Cs($6s$)-Xe pairs, respectively, relative to the $B\,^2\Sigma^+_{\frac{1}{2}}$ and $X\,^2\Sigma^+_{\frac{1}{2}}$ separated atom limits. Presuming the difference potential, $V_B(R) - V_X(R)$, to be a single-valued function of R, then the photoassociation wavelength $\lambda = hc\,[V_B(R) - V_X(R)]^{-1}$ uniquely specifies the position of the Franck-Condon region centered at R [16–18]. In the case of the Cs-Xe complex, the $B - X$ difference potential is a single-valued function of interatomic separation for $R \gtrsim 5.2$ Å.

A schematic diagram of the experimental arrangement is presented in Fig. 2. A dye laser, having a linewidth of ~ 0.05 cm^{-1} and pumped by the second harmonic (532 nm) of a Nd:YAG laser system, produces 8 ns (FWHM), linearly-polarized pulses (as indicated by the red dots in the figure) at a pulse repetition frequency of 10 Hz. After the pump laser pulse energy was sampled with detector 1, the pump beam propagated through a 50:50 nonpolarizing beam splitter (NPBS), followed by a quarter-wave plate, and entered a borosilicate glass cell situated in an oven and containing a mixture of an alkali vapor and research grade Xe. Depending on the orientation of the $\lambda/4$ plate, the pump polarization was either unaltered or converted to circular polarization. Separate cells were fabricated and filled for each alkali/Xe pressure combination but the length and diameter of the optical cell were fixed at 10 cm and 2.5 cm, respectively. Throughout the experiments, the Xe number density was set at either 1.9×10^{19} cm^{-3} or 2.6×10^{19} cm^{-3} which correspond (respectively) to gas pressures of 600 and 800 Torr at 300 K.

ASE is produced on the D_2 transition of Cs and Rb by the interaction of linearly or circularly-polarized pump pulses with the alkali vapor/Xe mixture. The backward-propagating ASE wave passes through the $\lambda/4$ plate and is partially reflected (50%) by the NPBS. A polarizing beam splitter (PBS) subsequently decomposes the ASE pulse into two orthogonal, linearly-polarized components. Calibrated detectors 2 and 3 measure, respectively, the absolute energies of the p-polarized and s-polarized pulses. The reliability and calibration of both detectors was verified by reversing their positions and confirming that the same results were obtained. If the incoming pulse is randomly polarized, detectors 2 and 3 measure the same pulse energy. Isolation of detectors 2 and 3 from scattered pump radiation was accomplished through optical layout and the insertion of D_2 line interference filters into the beam path.

Figure 3 presents excitation spectra obtained by photoassociating Cs-Xe thermal pairs with linearly-polarized laser pulses and recording the absolute energy of the ASE generated at 852.1 nm (Cs D_2 line) as the laser wavelength is scanned. Tuning the dye (pump) laser over the 838-850 nm region encompasses the Cs D_2 blue satellite ($B\,^2\Sigma_{\frac{1}{2}}^+ \longleftarrow X\,^2\Sigma_{\frac{1}{2}}^+$ transition of CsXe) which peaks at 842.7 nm. Throughout these experiments, the Cs and Xe number densities were fixed at 1.8×10^{15} cm^{-3} (T=473 K) and 2.6×10^{19} cm^{-3}, respectively, and the pump pulse energy was held constant at 1.6 mJ over the entire wavelength scan. Measurements of the ASE pulse energies, recorded by both detector 2 and detector 3, yield two spectra that are, as expected, identical because the incident optical field is linearly-polarized and the backward propagating ASE is randomly polarized. During this set of experiments, the $\lambda/4$ plate of Fig. 2 was oriented such that its fast axis was parallel to the pump polarization. Therefore, the $\lambda/4$ plate alters neither the linear polarization of the optical pump nor the random polarization of the generated ASE. Note, too, the absence of D_2 line ASE at (for example) 850 nm and 840 nm in Fig. 3, thus confirming effective rejection of scattered pump radiation by the measures described earlier.

If, however, the pump field is now circularly-polarized (σ^+), the spectra acquired with detectors 2 and 3 differ significantly, as shown in Fig. 4. Recorded under experimental conditions identical to those of Fig. 3 (except for the $\lambda/4$ plate orientation, discussed below), the excitation spectra of Fig. 4 demonstrate that the preponderance of the backward-propagating ASE generated by the σ^+ optical pump is also circularly-polarized but is polarized σ^- (i.e., opposite to that of the pump field). For example, the pulse energy recorded by detector 2 near the peak of the blue satellite (842.7 nm) constitutes more than 75% of the total ASE energy. An unexpected result is the difference between the spectral profiles of Fig. 4, which is particularly evident in the long wavelength
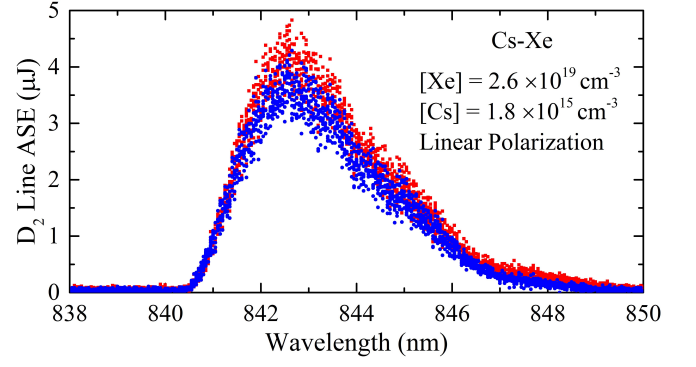

FIG. 3: Photoexcitation spectra recorded for Cs-Xe when the linearly-polarized pump is tuned over the $B\,^2\Sigma_{\frac{1}{2}}^+ \longleftarrow X\,^2\Sigma_{\frac{1}{2}}^+$ band of the diatomic complex (i.e., the D_2 blue satellite). Spectra acquired by monitoring the energy of detector 2 (red points) or detector 3 (blue) are identical.
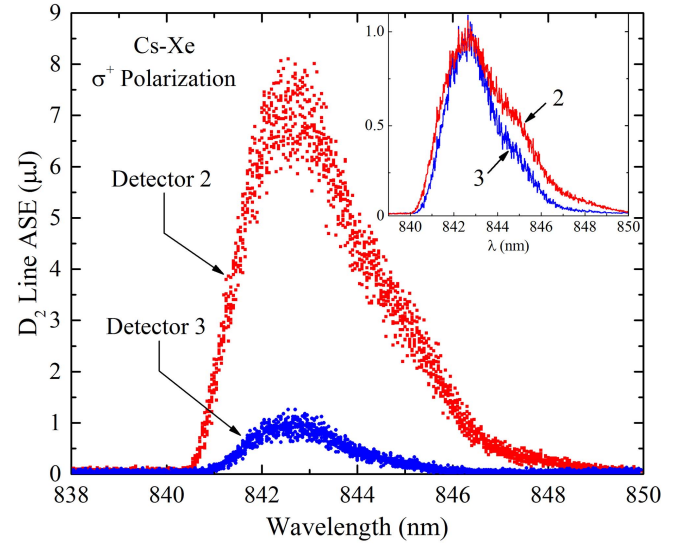

FIG. 4: Excitation spectra similar to those of Fig. 3 but recorded when the pump is circularly-polarized (σ^+). The inset compares the normalized profiles of both spectra.

portion of the blue satellite. To clarify this distinction, the inset to the figure compares the two spectra by scaling them such that their amplitudes match at the blue satellite peak. The spectral profile comparison of Fig. 4, resulting from multiple scans over the 843-850 nm wavelength region with a fixed pump laser energy, reveals a rapid decline in the production of unpolarized ASE (relative to the generation of σ^- radiation) when $\lambda \gtrsim 843.8$ nm. The difference between the two normalized spectra of Fig. 4 reaches maximum at ~ 845 nm. Before leaving this subject, a few comments regarding the role of the $\lambda/4$ plate are warranted. In these circularly-polarized pump experiments, the $\lambda/4$ plate was positioned with a precision stage such that its fast axis was rotated by 45° with respect to the pump polarization. Thus, the linearly-

polarized pump is, indeed, converted to σ^+ polarization. Because the backward-propagating ASE is predominantly polarized σ^-, this radiation is transformed by the $\lambda/4$ plate into linearly-polarized light, orthogonal to the polarization of the pump optical field, and is received by detector 2. The remaining, randomly-polarized, radiation is split equally between detectors 2 and 3.

The contribution of circularly-polarized radiation to the total ASE pulse energy cannot be calculated directly from the data of Fig. 4. Accordingly, a linear polarizer was inserted into the optical beam path of Fig. 2, immediately above the PBS. Monitoring the pulse energies recorded by detectors 2 and 3, as the linear polarizer was rotated in the plane transverse to the optical axis by a computer-controlled stage, yielded data such as those shown in Fig. 5(b) for $\lambda = 842.7$ nm. Measurements of the horizontally-polarized portion of the pulse energy as θ, the angle of the polarizer with respect to the vertical axis, was varied yields the data denoted by the red symbols. Corresponding measurements for the vertical polarization are illustrated in black. The data of Fig. 5(b) were analyzed by the matrix formalism of Jones [19] which allows for the polarization of the stimulated emission to be determined unambiguously. Representing the NPBS/linear polarizer/PBS combination by a 2×2 matrix results in the solid curves of Fig. 5(b) which represent the fit of the analysis of Ref. [19] to the data when circular polarization accounts for 65% of the ASE pulse energy. The remaining 35% of the ASE energy is randomly polarized. Data similar to those of Fig. 5(b), but acquired for different values of λ, yield the curve P(λ) in panel (a) of Fig. 5 which illustrates the variation with λ of the relative contribution of σ^--polarized ASE to the total pulse energy. It is immediately evident that polarizations approaching unity are observed at both the red and blue edges of the satellite spectrum (Fig. 5(a)) but the ASE is depolarized, relative to the pump, by almost 40% when the driving optical field wavelength is near the peak of the D$_2$ satellite.

We interpret the experimental results of Figs. 3-5 as demonstrating the spin polarization of Cs $6p\,^2P_{\frac{3}{2}}$ atoms by the dissociation of a transient diatomic molecule. Photoassociating alkali-rare gas atomic pairs through the free←—free, $B\,^2\Sigma^+_{\frac{1}{2}}$ ←— $X\,^2\Sigma^+_{\frac{1}{2}}$ transition with a circularly-polarized optical field excites the diatomic to the B state in a range of interatomic separation determined by λ. Subsequent dissociation of the $B\,^2\Sigma^+_{\frac{1}{2}}$ complex preferentially populates no more than two hyperfine levels of the Cs $6p\,^2P_{\frac{3}{2}}$ state ($F = 4, 5$). This conclusion is supported by measurements comparing the D$_2$ line (852.1 nm) ASE pulse energy generated when the pump field polarization is circular or linear. Specifically, the threshold pump pulse energy for the appearance of σ^--polarized ASE is 0.30 ± 0.03 mJ/pulse for Cs-Xe, or approximately 2/3 of that for the production of unpolar-
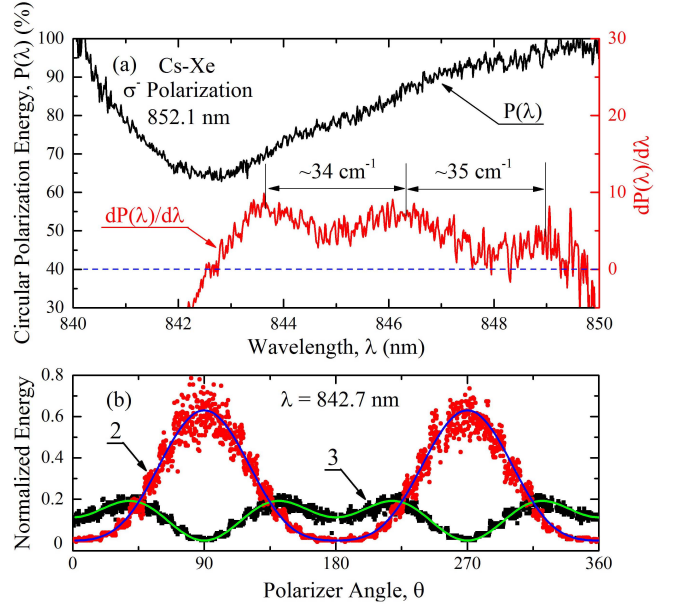

FIG. 5: (a) (Black) P(λ): Dependence on pump wavelength of the contribution of σ^- polarized ASE (at 852.1 nm) to the total energy of the backward-propagating pulse; (Red) Derivative of P(λ) with respect to λ in the 842-850 nm interval which corresponds to $5.3 \lesssim R \lesssim 6.2$ Å. (b) Polarization data obtained for $\lambda = 842.7$ nm by detectors 2 (horizontal) and 3 (vertical).

ized ASE (0.45 ± 0.03 mJ/pulse). This measured ratio for threshold pump energies is consistent with the reduction in the effective degeneracy g of the Cs $6p\,^2P_{\frac{3}{2}}$ state resulting from populating only the $F = 4, 5$ hyperfine sublevels (with a σ^+-polarized pump), as opposed to populating all four hyperfine levels ($F = 2 - 5$) with a linearly-polarized pump. If the thermalized populations of the Cs $6s\,^2S_{\frac{1}{2}}$ ($F = 3, 4$) states are preserved during the dissociation of CsXe(B), then the normalized, relative populations of the Cs $6p\,^2P_{\frac{3}{2}}$ $F = 4$ and 5 hyperfine levels can be presumed to be $\sim 45\%$ and $\sim 55\%$, respectively. It should also be noted that radiation trapping of the alkali D$_2$ line ASE is not expected to influence the data significantly, owing to saturation of the alkali-rare gas B ←— X transition by the pump optical field.

As noted earlier, the $B\,^2\Sigma^+_{\frac{1}{2}}$ potential of the alkali-rare gas diatomics is best described by Hund's case (b) coupling in which the spin vector $\vec{S}$ is orthogonal to the internuclear axis. In addition, the electronic orbital angular momentum precesses at 90° to the internuclear axis and, therefore, a magnetic moment $\vec{\mu}$, also oriented at a right angle to the axis [20], is established. It appears that the unique structural characteristics of the $^2\Sigma^+_{\frac{1}{2}}$ state (indeed, all $^2\Sigma$ states) are responsible for the high degree of spin polarization of the Cs fragment of the CsXe(B) dissociation process, despite the absence of an external magnetic field. Any explanation for the experimental re-

sults of Figs. 3-5, however, must account for the clear difference between the spectral profiles associated with circularly-polarized and unpolarized ASE. Specifically, the partial depolarization of the ASE in Fig. 4, most pronounced in the $\lambda = 841 - 846$ nm region, appears to arise from a localized modification in the molecular orbital structure of the $B\,^2\Sigma_{\frac{1}{2}}^+$ state. Calculations of the B and X potentials on the basis of experimental absorption spectra [14] are in agreement with previous theoretical work [21, 22] in predicting the difference potential, $V_B(R) - V_X(R)$, to be single-valued for $R \gtrsim 5.2$ Å and the peak of the barrier in the $B\,^2\Sigma^+$ potential (Fig. 1) to lie at approximately 5.3 Å. Consequently, the photoexcitation of Cs-Xe ground state pairs in the $841 - 846$ nm pump wavelength interval (i.e., in the vicinity of the blue satellite peak) corresponds to the formation of CsXe(B) molecules directly atop the barrier and along its outer wall (to $R \sim 6$ Å). In 1974, Pascale and Vandeplanque [13] predicted the existence of the $B\,^2\Sigma_{\frac{1}{2}}^+$ barrier (at ~ 4.5 Å). They attributed the potential "hump" to coupling of the B state of the Cs-rare gas diatomics with $\Omega = \frac{1}{2}$ potentials derived from Cs($5d$)+Rg($^1S_0$). Although Nakatsuji and Ehara [21] subsequently affirmed (from calculations) the existence of a barrier in the CsXe $B\,^2\Sigma^+$ state and observed configuration mixing involving the $5d$ potentials, no experimental verification of this interaction has been reported.

We interpret the partial depolarization of the D_2 line ASE in Fig. 5(a) as arising from the interaction of the $6p\sigma$ antibonding molecular orbital (MO) of the $B\,^2\Sigma_{\frac{1}{2}}^+$ state with a $5d\sigma$ MO in the $R \approx 5-6$ Å region. An unexpected result from these experiments is that the perturbation of the $B\,^2\Sigma_{\frac{1}{2}}^+$ potential is sufficient to significantly reduce the degree of Cs $6\,^2P_{\frac{3}{2}}$ spin polarization. A spectroscopic probe of R-dependent perturbations of a molecular state has been realized by combining circularly-polarized photoexcitation of a transient diatomic with analysis of the polarization of the resulting ASE. Recently, the detection of diatomic potential energy barriers only a few cm^{-1} in height was reported [15] but weak state-state interactions can now be probed in a collisional environment by analysis of electronic spin polarization. Further evidence for this interpretation of the experimental data is provided by the lower of the two spectra in Fig. 5(a). If P(λ) (black trace) can be understood as a relative measure of the strength of the $6p\sigma - 5d\sigma$ interaction, then the derivative dP(λ)/dλ (red profile, Fig. 5(a)) shows the perturbation magnitude in this region of R to oscillate with a periodicity of 35 ± 2 cm^{-1} which is quite close to the vibrational frequencies calculated in Ref. [22] for the $5d\Pi$ and Δ states of CsXe. It is reasonable to conclude that the dependence of Cs $6p\,^2P$ spin polarization on photoassociation wavelength provides a spectroscopic diagnostic of the alteration of $^2\Sigma_{\frac{1}{2}}^+$ structure brought about by an interaction with the lowest vibrational levels of a $5d\,^2\Lambda_{\frac{1}{2}}$ ($\Lambda = 1$ or 2) state.

In summary, electronic spin polarization of Cs $6p\,^2P_{\frac{3}{2}}$ atoms has been demonstrated in the absence of an external magnetic field by photoexciting a transient diatomic molecule with a circularly-polarized optical field. As opposed to the polarization of the $ns\,^2S_{\frac{1}{2}}$ alkali ground state by the prevalent depopulation method, polarization is produced in an alkali atomic excited state, and monitored by ASE. Forming Cs-rare gas excited diatomic molecules at or near the peak of the $B\,^2\Sigma_{\frac{1}{2}}^+$ barrier by photoassociation controls the degree of Cs($6p$) spin polarization, an observation attributed to the influence on the B state $6p\sigma$ antibonding MO by a $5d\sigma$ MO associated with a higher-lying electronic state correlated with Cs($5d$)+Xe. Consequently, weak electronic interactions influencing a dissociative interatomic potential are capable of profoundly impacting the spin polarization of the alkali photofragment. These results provide the basis for a laser spectroscopic technique able to probe state-state interactions with interatomic separation (R) resolution. From an applied perspective, the ability to vary, on a continuous basis, the degree of spin polarization through the wavelength of the optical field offers a tool for surface physics and MRI imaging studies. Furthermore, since Xe is a participant in the excited alkali atom generation process, experiments similar to those reported here with ^{129}Xe may demonstrate an increased rate for producing hyperpolarized ^{129}Xe atoms relative to the conventional approach of photoexciting the alkali directly.

---

* Electronic address: mironov.mae@gmail.com
[1] W. Happer, Rev. Mod. Phys. **44**, 169 (1972).
[2] I. K. Kominis, T. W. Kornack, J. C. Allred, and M. V. Romalis, Nature **422**, 596 (2003).
[3] V. Shah, S. Knappe, P. D. D. Schwindt, and J. Kitching, Nature Photon. **1**, 649 (2007).
[4] A. Hartung, F. Morales, M. Kunitski, K. Henrichs, A. Laucke, M. Richter, T. Jahnke, A. Kalinin, M. Schöffler, L. P. H. Schmidt, M. Ivanov, O. Smirnova, and R. Dörner, Nat. Photon. **10**, 526 (2016).
[5] J. C. Kemp, J. H. Macek, and F. W. Nehring, Astrophys. J. **278**, 863 (1984).
[6] M. A. Bouchiat, T. R. Carver, and C. M. Varnum, Phys. Rev. Lett. **5**, 373 (1960).
[7] W. Happer, E. Miron, S. Schaefer, D. Schreiber, W. A. van Wijngaarden, and X. Zeng, Phys. Rev. A **29**, 3092 (1984).
[8] W. Hanle, Z. Physik **30**, 93 (1924).
[9] H. G. Dehmelt, Phys. Rev. **105**, 1487 (1957).
[10] T. G. Walker and W. Happer, Rev. Mod. Phys. **69**, 629

(1997).

[11] N. Whiting, N. A. Eschmann, B. M. Goodson, and M. J. Barlow, Phys. Rev. A **83**, 053428 (2011).

[12] M. G. Shapiro, R. M. Ramirez, L. J. Sperling, G. Sun, J. Sun, A. Pines, D. V. Schaffer, and V. S. Bajaj, Nature Chemistry **6**, 629 (2014).

[13] J. Pascale and J. Vandeplanque, J. Chem. Phys. **60**, 2278 (1974).

[14] J. D. Hewitt, A. E. Mironov, and J. G. Eden (unpublished).

[15] A. E. Mironov, W. Goldshlag, and J. G. Eden, Appl. Phys. Lett. **107**, 041112 (2015).

[16] A. Jabloński, Phys. Rev. **68**, 78 (1945).

[17] R. E. M. Hedges, D. L. Drummond, and A. Gallagher,

[18] J. Tellinghuisen, *in Photodissociation and Photoionization*, edited by K. P. Lawley, Advances in Chemical Physics, Vol. LX (Wiley, New York, 1985) pp. 299-369.

[19] R. C. Jones, J. Opt. Soc. Am. **31**, 488 (1941).

[20] G. Herzberg, *Molecular Spectra and Molecular Structure*, Vol. I. Spectra of Diatomic Molecules (Van Nostrand Reinhold Company, New York, 1950).

[21] H. Nakatsuji and M. Ehara, Chem. Phys. Lett. **172**, 261 (1990).

[22] M. Ehara and H. Nakatsuji, J. Chem. Phys. **102**, 6822 (1995)
.

Phys. Rev. A **6**, 1519 (1972).